doi.org/10.52568/000624/JCSP/42.02.2020

Structural, Topographical and Optoelectronic Properties of $ZnIn_2S_4$ Thin Films Deposited from Dual Source Using Aerosol Assisted Chemical Vapour Deposition (AACVD) Technique

[1,2] Umar Daraz, [1]Tariq Mahmood Ansari*, [3]Shafique Ahmad Arain,
[2,4] Muhammad Adil Mansoor and [5]Muhammad Mazhar
[1]*Institute of Chemical Sciences, Bahauddin Zakariya University, Multan 60800, Pakistan.*
[2]*Department of Chemistry, Faculty of Science, University of Malaya, 50603, Kuala Lumpur, Malaysia.*
[3]*Institute of Chemistry, Shah Abdul Latif University Khairpur, Sindh, Pakistan.*
[4]*Department of Chemistry, School of Natural Sciences (SNS), National University of Science and Technology, H-12, Islamabad, Pakistan.*
[5]*Department of Environmental Sciences, Fatima Jinnah Women University, The Mall, Rawalpindi, Pakistan.*
tariqansari@bzu.edu.pk*

(Received on 22nd October 2018, accepted in revised form 17th May 2019)

Summary: The $ZnIn_2S_4$ (ZIS) thin films have been successfully developed from a homogeneous toluene solution of dithiocarbamate complexes of zinc and indium with formula $[Zn(S_2CNCy_2)_2(py)]$ **(1)** and $[In(S_2CNCy_2)_3].2py$ **(2)** via aerosol assisted chemical vapor deposition (AACVD) technique. Deposition experiments were carried out at 500°C in an inert atmosphere of argon gas on FTO substrate. The X-ray diffraction (XRD), X-ray photoelectron spectroscopy (XPS), field emission scanning electron microscopy (FESEM) and Raman spectroscopy have been used for the determination of phase purity, surface topography of the uniformly distributed particles and oxidation states of the elements present in thin films. Further UV-visible spectrophotometry elucidates that the thin films absorbs in entire visible region and give estimated band gap energy of 2.37 eV. The photoelectrochemical (PEC) response in terms of linear scan voltammetry (LSV) provides a photocurrent density 2.27 $mA.cm^{-2}$ at 0.7 V vs Ag/AgCl/3M KCl using 0.05 M sodium sulphide solution under AM 1.5 G illumination (100 $mW.cm^{-2}$). The LSV results are further reinforced by electrochemical impedance spectroscopy (EIS) that gives charge transfer resistance (R_{ct}) value of 5.7 x 10^4 Ω under dark conditions and reduces to 3.7 x 10^4 Ω under illumination.

Keyword: $ZnIn_2S_4$; Thin film; Photo oxidation of water; Band gap; Photoconductivity.

Introduction

The story of photocatalyst began with the development of titanium oxide (TiO_2) back in 1972. Since then photocatalyst technology has been used as an alternative energy source for natural resources [1-3]. This technology helps to generate hydrogen by photolytic water splitting and also serves as green energy source by destroying pollutants in water under normal conditions of temperature and pressure [4, 5]. Numerous metal oxides and metal sulphides had been synthesized and applied as photocatalyst in past but the later has an advantage due to high conduction band value and utilization of visible portion of solar spectrum [6-8]. Therefore, metal sulphide are best choice for scientists due to better visible and UV radiation response[9-11].

Owing to semiconducting nature, low band gap of 2.3-2.5 eV and chemical stability, $ZnIn_2S_4$ has gained much attention towards exploring new grounds in field of solar cell applications and photooxidation of water for hydrogen production [11-17]. Moreover, $ZnIn_2S_4$ is a ternary chalcogenide semiconductive material having layered alignment and finds extensive functions in optical and photoconductive devices [18-24]. Various $ZnIn_2S_4$ nanostructures and microstructures, such as, nanoribbon, nanotubes, nanoplate, sub microsphere and nanowire have been synthesized via different techniques [13, 23, 25-31]. But still tailoring of $ZnIn_2S_4$ thin films with nanostructure and uniform distribution is a big challenge that bounds their utilization in photovoltaic devices. Various physical and chemical methods with their own pros and cons have been used for deposition of $ZnIn_2S_4$ thin films. These techniques involve MOCVD [32], SILAR [33], hydrothermal method [18], electrodeposition [34], chemical bath deposition [35], atomic layer deposition [36], microwave assisted synthesis [37], spin coating method [38] and spray pyrolysis method.[39] Due to some limitations pertaining to afore mentioned techniques such as utilization of expensive instruments, requisite of line of sight between source and substrate, requirement of high vacuum, low deposition rate, low morphological control, low purity of product, difficulty in

*To whom all correspondence should be addressed.

controlling metal ions ratio, etc.[40], we therefore, focused on developing the thin films via AACVD.

The thin film deposition technique (AACVD) using single and mixed molecular precursors attracted the attention of researchers in recent years as this method is simple and scalable. Moreover, particle size and morphology of the deposited thin films can easily be controlled by varying different parameters such as deposition temperature, solvent choice and frequency of ultrasonic modulator[41]. Many nano scaled thin films of metal sulphide using single source metal dithiocarbamate precursor have been synthesized and reported in past few years such as indium sulphide [42], zinc sulphide[43], cadmium sulphide[44], bismuth sulphide[45] and silver sulphide[46]. Recently AACVD technique has been used to fabricate ZnO thin films on FTO glass substrate [47-48]. But deposition of $ZnIn_2S_4$ thin films by AACVD is not reported to date. Since both the precursors (**1**) and **(2)** have very similar salvation and thermal properties [42, 43],therefore we were prompted to synthesize $ZnIn_2S_4$ using their (1:2) solution in toluene to fabricate thin films on FTO substrate at 500°C. The synthesized $ZnIn_2S_4$ thin films were characterized by XRD, XPS, EDX, FESEM, Raman and UV-Vis spectroscopy for their crystallinity, structure, topographic morphology, oxidation state of elements involved, phase purity, and optical band gape values. Moreover, photoconductive characteristics of fabricated $ZnIn_2S_4$ thin films measured by linear scan voltammetry and supported by impedance results, confirmed that the films are active for solar light harvesting applications.

Experimental

Synthesis of $[Zn(S_2CNCy_2)_2(py)]$ (1) and $[In(S_2CNCy_2)_3].2py$ **(2)**

The precursor complexes $[Zn(S_2CNCy_2)_2(py)]$ **(1)** and $[In(S_2CNCy_2)_3].2py$ **(2)** were synthesized by following the reported procedure as described below[42, 43].

The 0.75 g (2.7 mmol) of purified crystals of $Na(S_2CNCy_2)$ were dissolved in chloroform in a round bottom flask fitted with a reflux condenser, a dropping funnel and inert gas line. To this stirring solution was added about 0.18 g (1.32 mmol) of zinc chloride that made the solution turbid. After half an hour stirring, pyridine was added dropwise to this turbid mixture that resulted in a clear solution. After 2 hours stirring the solution was kept for crystallization in the fume hood, that yielded colorless crystals of $[Zn(S_2CNCy_2)_2(py)]$ **(1)** after evaporation of solvent.[2] Same procedure was applied for the synthesis of indium complex, except that in synthesis of **(2)** methanol was used as solvent rather than chloroform and 0.195 g (0.9 mmol) of indium trichloride was used to get colorless crystals of $[In(S_2CNCy_2)_3].2py$ **(2).**[1]

Fabrication of thin films

The $ZnIn_2S_4$ thin films were fabricated from $[Zn(S_2CNCy_2)_2(py)]$ **(1)** and $[In(S_2CNCy_2)_3].2py$ **(2)** at 500 °C on FTO glass substrate via AACVD technique explained elsewhere.[1] The FTO coated glass substrate with dimension 25.4 x 12.7 x 2.2 mm (L x W x D) and surface resistivity of 7 Ω/sq were ultrasonically cleaned with ethanol and acetone and finally rinsed with distilled water prior to fabricate the thin films. In normal deposition procedure, 0.1 g (0.152 mmoles) of $[Zn(S_2CNCy_2)_2(py)]$ **(1)** and 0.316 g (0.303 mmoles) of $[In(S_2CNCy_2)_3].2py$ **(2)** were dissolved in 10 ml toluene solvent and then transferred to a 50 ml round-bottomed flask associated with deposition arrangements. The FTO substrates were placed in a reactor tube and argon as a carrier gas was flow at rate of 100 $mL.min^{-1}$. The temperature of substrates inside reactor tube was adjusted to 500 °C about ten minutes before the agitation of precursor solution for aerosol generation. A piezoelectric modulator of an ultrasonic humidifier was used to agitate the precursor's solution in a round bottom flask to produce the aerosols. The carrier gas then moved the aerosol to hot reactor tube where aerosols decomposed to produce targeted ZIS thin films on FTO substrates. The total time for deposition of film was 40 minutes. During the experiment the exhaust and volatiles from the reactor tube was extracted into extraction system inside fuming hood. Finally, the films were allowed to cool at room temperature under continuous flow of argon gas, prior to use them for characterization and PEC studies. The deposition experiment was repeated several times to confirm the reproducibility of fabricated films.

Characterization of Materials

Field emission gun electron microscope, FESEM (FEI Quanta 400) integrated with energy dispersive X-rays spectrometer (EDX-INCA Energy 200) was used to evaluate elemental composition and morphological aspects of ZIS thin films under controlled settings of accelerating voltage (20 kV) with a working distance (9.2 mm). The PAN analytical diffractometer (X'Pert High Score) with high intensity monochromatic radiation of Cu-Kα having wavelength (λ) 1.54184 Å was employed to

elucidate crystalline phase and crystallinity of synthesized ZIS thin films. In order to screen all conceivable reflection peaks, the test materials (Thin films) were scanned from 10° to 60° with a step size of 0.026° operating at 40 kV and 40 mA. The Raman spectroscopical analysis was performed with Raman microscope (Renishaw InVia) and a beam of argon laser (514 nm) of output power (0.01 mW) was used to excite the samples. The X-ray photo electron spectroscopic (XPS) studies of ZIS thin films were achieved on ULVAC-PHI (Quantera II) having monochromatic radiation of Al Kα (1486.8 eV) as X-rays donor operating at 25.6 W. The narrow scan analysis was done by using an energy source of 112 eV with 0.1 eV at every step. The UV-vis spectrophotometer (Lambda 35 Perkin-Elmer) was used to estimate light absorbing capacity (optical absorbance) of fabricated ZIS thin films.

The data were gathered in the wavelength range of 350 to 900 nm applying pure FTO glass substrate as a reference electrode. The thickness of $ZnIn_2S_4$ films is determined by using a profilometer KLA Tencore P-6 surface profiler.

The photoelectrochemical (PEC) behavior of $ZnIn_2S_4$ thin films was assessed by employing an electrochemical cell consisting of three electrodes and having a quartz window. This standard electrochemical cell uses Ag/AgCl.3M KCl as a reference electrode, platinum wire as a counter electrode and an aqueous solution Na_2S (0.01M) as an electrolyte to measure the photoconductive response of $ZnIn_2S_4$ films electrodes. The solar simulator AM 1.5 (Solar Light 16S-300 solar simulator) was use to illuminate the cell's compartment throughout the experiments with intense light of 100 $mWcm^{-2}$ and the operative range of electrodes was 1 cm^2. The PEC response interms of steady state current-voltage (I-V Curves) and electrochemical impedance spectroscopy (EIS) was recorded on potentiostat Autolab type III (Eco Chemie micro).

Results and Discussion

The precursors $[Zn(S_2CNCy_2)_2(py)]$ **(1)** and $[In(S_2CNCy_2)_3].2py$ **(2)** are obtained in 75% and 80% yield by double displacement reaction of $\{Na(S_2CNCy_2)\}$ with zinc chloride and indium chloride in pyridine-chloroform and pyridine-methanol solvent system, respectively. The synthesized precursors contain pyridine as Lewis base that promotes its stability at room temperature, resistance to air and moisture, and ease of solubility in suitable organic solvents. Furthermore, both of the precursors (1) and (2) are soluble in common organic solvents such as chloroform, THF, pyridine and toluene and give stable sulphide after decomposition at 400 °C and above [42, 49]. Keeping in view these similar dissolution and thermal properties such as decomposition temperature (375 °C for **(1)** and 340 °C for **(2)**), $ZnIn_2S_4$ thin films were fabricated at 500 °C using the stoichiometric ratio of precursors in toluene solution.

X-Ray Diffraction Studies

Crystalline phase, degree of crystallinity and phase purity of the ZIS thin films fabricated at 500°C on FTO substrate was evaluated by using X- ray diffraction spectroscopy (XRD) and results are depicted in Fig. 1. The XRD pattern obtained is in good agreement with that of hexagonal $ZnIn_2S_4$ nano-sheets reported by Zhenyi *et al* [50]. The relative peak positions labelled by (■) at 2θ value of 21.1, 26.8, 28.3, 41.2, 47.2, 52.8° belongs to (006), (102), (104), (108), (110) and (116) lattice respect of phase pure $ZnIn_2S_4$. Whereas, the remaining peaks marked by (▼) are originated from fluorine doped tin oxide (FTO) substrate and the two peaks at 2θ value of 33.6 and 56.2° are shared by both $ZnIn_2S_4$ and FTO. The thickness of films is 410 nm as determined by profilometer. It is clear from the diffractogram that we have got better pattern of hexagonal phase of $ZnIn_2S_4$ interms of peak intensities and peak broadening as compared to that of previously reported and this might be attributed to the well-defined and uniform distribution of end product on the surface of substrate as supported by FESEM studies.

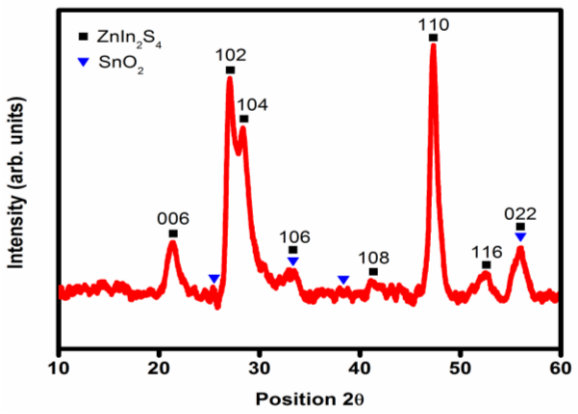

Fig. 1 XRD pattern of $ZnIn_2S_4$ thin films fabricated from homogenous solution of precursors (1) and (2) at 500 °C on FTO substrate via AACVD.

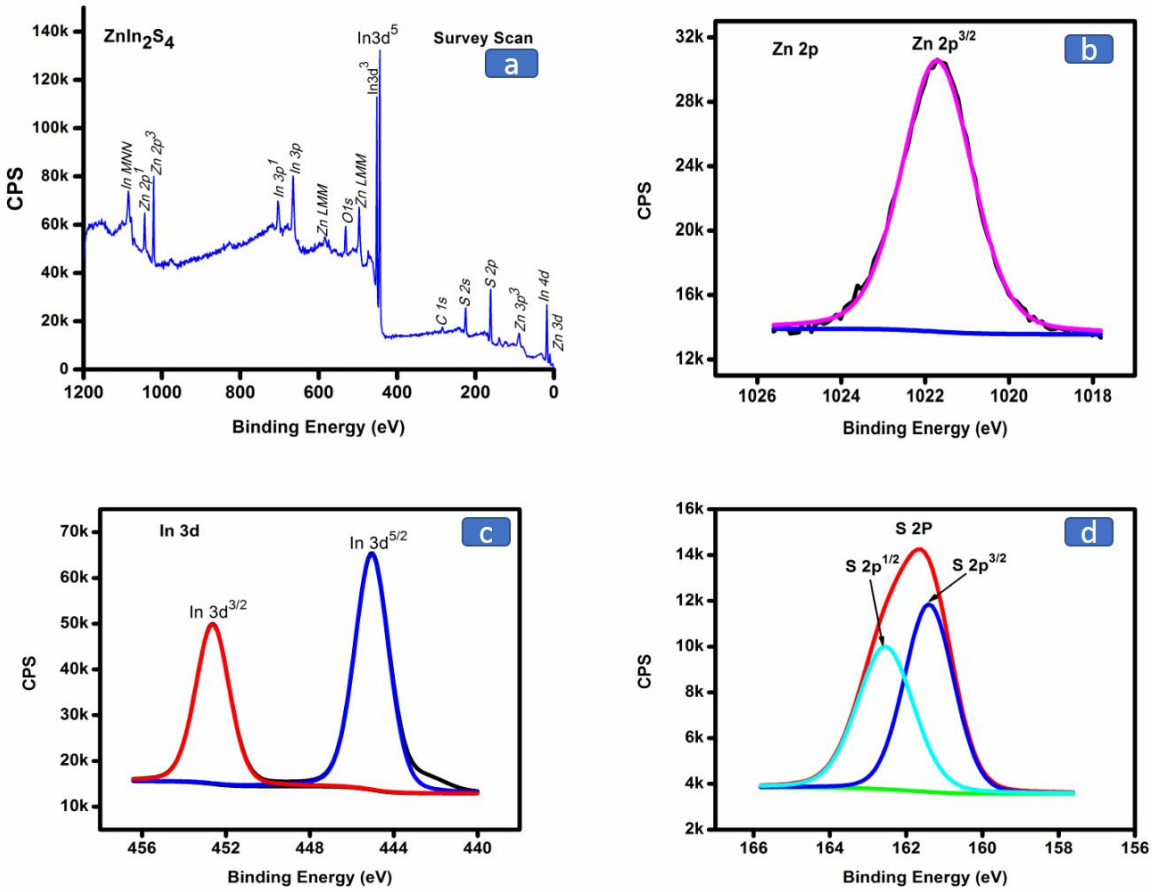

Fig. 2 XPS spectra of $ZnIn_2S_4$ thin films fabricated on FTO at 500 ºC using toluene solution of precursor (1) and (2) (a) Survey scan (b) Zn 2p ^{3} (c) In 3d ^{5} and (d) S 2p.

XPS Analysis

To verify XRD results, the X-ray photoelectron spectroscopic (XPS) analysis (Fig. 2) was carried out to determine elemental composition and oxidation state of elements present in $ZnIn_2S_4$ thin films. The survey scan spectrum (Fig. 2a) confirms that Zn, In and S are major components at the surface of films as indicated by the peaks of binding energies (eV) 87.85, 492.87, 585.03, 1021.66, 1043.44 for Zn, 17.47, 443.95, 452.51, 666.23, 702.88, 1085.28 for In and 161.76, 225.08 for S. The one peak appears at 531 eV is due to the contribution of FTO substrate. Moreover, the atomic ratio of Zn, In and S, provided by XPS is almost 1:2:4 and is good agreement with the results obtained from EDX analysis (ESI Fig. 1†), thereby confirming the fabrication of phase pure $ZnIn_2S_4$ thin films.

The narrow scan spectrum of Zn (Fig. 2b), shows peak at 1021.7 eV corresponds to the binding energy of $Zn2p_{3/2}$ [51], for In (Fig. 2c) there appears two peaks at 444.7 eV and 452.3 eV with separation energy of 7.6 eV belong to binding energy of $In3d_{5/2}$ and $In3d_{3/2}$ respectively confirms that indium is present in oxidation state of +3, while the spectrum of Sulphur (Fig. 2d) gives two peaks at 161.3 eV and 162.5 eV that corresponds to binding energy of S2p [52].

Raman Spectroscopy

Further to support XRD and XPS results, $ZnIn_2S_4$ thin films were subjected to Raman spectroscopic analysis for its microstructural analysis (Fig. 3). Raman spectroscopical analysis is very good technique to assess the crystallinity of target materials as it offers inelastic distribution of peaks that furnish knowledge about vibration modes of crystalline material. The semiconductive material of good crystallinity presents the more intense Raman modes in comparison to the poor crystalline materials. The Raman spectra of fabricated ZIS thin films (Fig. 3) presents peaks at 248.1(longitudinal mode), 308(transverse mode) and 359.2 cm^{-1}(longitudinal mode), which are in very close match with previously reported Raman results of $ZnIn_2S_4$ semiconductor[38].

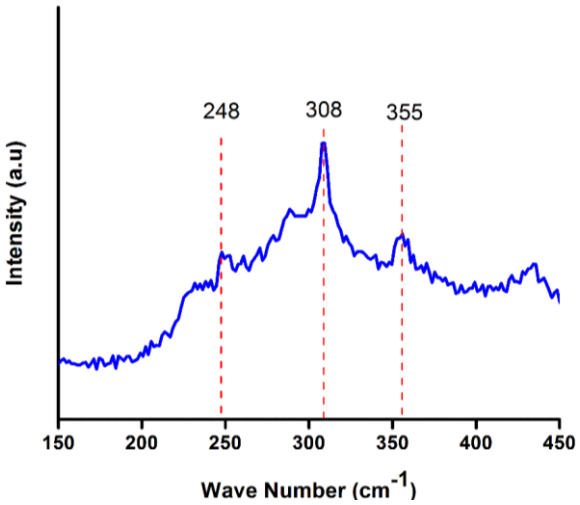

Fig. 3: Raman scattering of $ZnIn_2S_4$ thin films fabricated on FTO substrate at 500 ºC from toluene solution of precursors **(1)** and **(2)** via AACVD.

Topographical Analysis

The surface morphology of deposited $ZnIn_2S_4$ thin films on FTO substrate at 500ºC was determined by using FESEM analysis. The thin film surface morphology (Fig. 4) elucidates uniformly distributed irregular shaped compact particles having well-defined sharp boundaries. The well-connected particles with some voids entirely covered the surface of FTO substrate which can facilitate the electrolyte to penetrate and interact the inner layers of thin film once stimulates by sunlight.

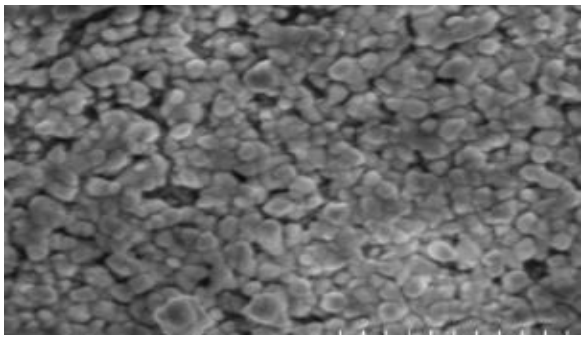

Fig. 4: FESEM image of $ZnIn_2S_4$ thin films developed from toluene solution of precursors (1) and (2) at temperature of 500 ºC by AACVD.

Optical studies

The optical band gap energy of $ZnIn_2S_4$thin film was retrieved from UV-Vis spectrum (Fig 5). The UV-vis spectrum of thin film shows a steady increase in absorbance while moving towards lower wavelength of light and approaches to its maximum value at 380 nm. The optical band gap (E_g) values were obtained from Tauc's equation:

$$\alpha h\nu = A\,(h\nu - E_g)^{\gamma}$$

where α is the linear absorption coefficient of the material, $h\nu$ is the photon energy, A is a proportionality constant and γ is a constant depending on the band gap nature; γ = 1/2 for allowed direct band gap and γ = 2 for indirect band gap. The direct band gap was calculated by using Tauc's equation arranged as $(\alpha h\nu)^2 = A_1(h\nu - E_g)$. A plot of $(\alpha h\nu)^2$ versus $h\nu$ (Inset of Fig. 5) gave a linear region with slope A_1 whose extrapolation to $\alpha(h\nu) = 0$ would yield the value of the direct band gap of 2.37 eV for $ZnIn_2S_4$ thin films fabricated at 500 ºC from toluene solution of precursors **(1)** and **(2)** of FTO substrate. This band gap value is in good agreement with reported values[16].

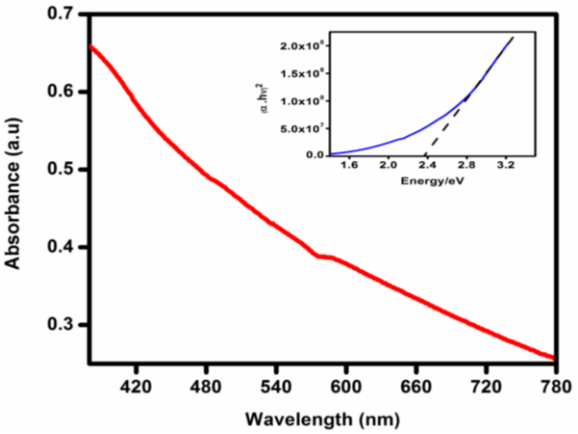

Fig. 5: UV-Visible spectrum of $ZnIn_2S_4$ thin films fabricated on FTO substrate at 500 ºC in toluene solution of precursors (1) and (2) and inset is the Tauc's plot giving optical band gap value of 2.37 eV for $ZnIn_2S_4$ thin films.

Photo-electrochemical Response

The Linear Scan Voltammetry (LSV) of $ZnIn_2S_4$ thin films (Fig. 6), performed in 0.01 M Na_2S aqueous solution, produces anodic photocurrent density of 2.27 $mA.cm^{-2}$ at + 0.7 V. It is found that the photocurrent density produced in present studies is higher as compared to the previously reported photocurrent density values of 8 $\mu A.cm^{-2}$ and 1.5 $mA.cm^{-2}$ for ZnS and In_2S_3 thin films, respectively. Moreover, it is revealed that this value is also higher

than the previously reported photocurrent density of 0.27 mA.cm^{-2} and 0.29 mA.cm^{-2} [33, 38, 39] for single phase $ZnIn_2S_4$ produced by different techniques. This improvement in photocurrent density is attributed to uniform distribution of particles with a porous texture. The porous texture of thin film facilitates the electrolyte to penetrate deep into the inner layers and increase the electrode-electrolyte surface interaction. At the same time well-connected particles make an ease to electronic flow.

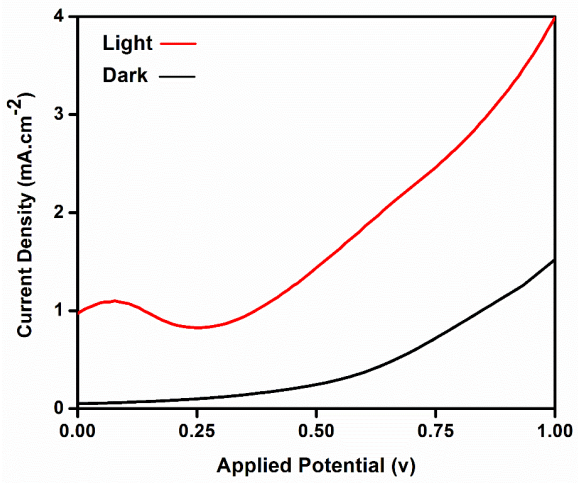

Fig. 6 Linear sweep voltammetry (LSV) of $ZnIn_2S_4$ thin films fabricated on FTO substrate at 500 ^oC in toluene solution of precursors (1) and (2) in dark (black) and under light (red).

Moreover, the ZIS thin films were subjected to electrochemical impedance spectroscopical (EIS) analysis in order to get improved vision of interfacial charge transport resistance between electrode face and electrolyte and outcomes are depicted in Fig. 7. The Nyquist plots of $ZnIn_2S_4$ thin films under dark and illumination (Fig. 7) showed the equivalent series resistance (R_s) of device which is obtained when high frequency semicircles intersect the x-axis. Herein, the R_s value can be overlooked as it remains almost same in light and dark situations due to similar material nature. The simulated semicircles under light and dark (inset of figure 7) provide charge transfer resistance (R_{ct}) values. It is observed that the R_{ct} value of $ZnIn_2S_4$ thin film decreases significantly from 5.7 x $10^4\Omega$ to 3.7 x 10^4 Ω after light illumination indicating an ease in electron transport with minimum possibility of the charge recombination, thus delivering enhanced photocurrent density and photoresponse for oxidation of water.

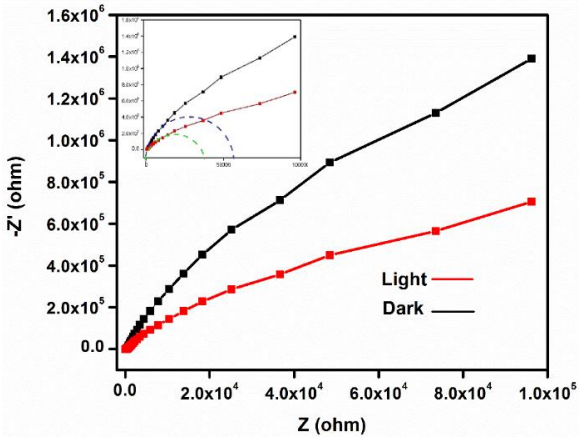

Fig. 7 Nyquist plot of $ZnIn_2S_4$ thin films fabricated on FTO substrate at 500 ^oC in toluene solution of precursors (1) and (2) in dark (black) and under light (red).

Conclusions

In summary, Zinc thioindate thin films are successfully fabricated on FTO substrate at 500 ^oC from dual source precursors **(1)** and **(2)** possessing similar physicochemical properties by Aerosol Assisted Chemical Vapor deposition (AACVD) method and used as photoelectrode. It is found that well connected particles of the thin films with porous texture and a band gap of 2.37 eV provide exceptionally improved photocurrent density of 2.27 mA.cm^{-2} which was further confirmed by impedance studies. The Nyquist curves show a prominent shift of charge transfer resistance from $5.7 \times 10^4\ \Omega$ to $3.7 \times 10^4\ \Omega$ under illumination and approve the improvement in charge transfer under light conditions. These results indicate the utilization of these ternary thin films in photovoltaic and photoelectrochemical devices.

Acknowledgment

This paper is a part of PhD thesis of Mr. Umar Daraz. Umar Daraz is highly thankful to the Higher Education Commission, Islamabad, Pakistan for financial support under the International Research Support Initiative Programme (IRSIP). Authors are highly obliged to the Institute of Chemical Sciences, Bahauddin Zakariya University, Multan Pakistan and the University of Malaya, Kuala Lampur, Malaysia for providing laboratory and instrumental facilities to carry out these investigations.

Conflict of interest

The authors have no conflict of interests.

References

1. O. Ellabban, H. Abu-Rub, F. Blaabjerg, Renewable energy resources: Current status, future prospects and their enabling technology, *Renew. Sustain. Energy Rev.*, **39,** 748 (2014).
2. H. Tong, S. Ouyang, Y. Bi, N. Umezawa, M. Oshikiri, J. Ye, Nano-photocatalytic materials: possibilities and challenges, *Adv. Mater.*, **24**, 229 (2012).
3. X. Chen, L. Li, W. Zhang, Y. Li, Q. Song, L. Dong, Fabricate Globular Flower-like CuS/$CdIn_2S_4$/$ZnIn_2S_4$ with High Visible Light Response via Microwave-assisted One–step Method and Its Multipathway Photoelectron Migration Properties for Hydrogen Evolution and Pollutant Degradation, *ACS Sustainable Chem. Eng.*, **4,** 6680 (2016).
4. S. Protti, A. Albini, N. Serpone, Photocatalytic generation of solar fuels from the reduction of H_2O and CO_2: a look at the patent literature, *Phys. Chem. Chem. Phys.*, **16**, 19790 (2014).
5. C. Wang, J.-R. Li, X.-L. Lv, Y.-Q. Zhang, G. Guo, Photocatalytic organic pollutants degradation in metal–organic frameworks, *Energy Environ. Sci.*, **7,** 2831 (2014).
6. W. Chen, G.-R. Duan, T.-Y. Liu, Z.-M. Jia, X.-H. Liu, S.-M. Chen, X.-J. Yang, Synthesis of homogeneous one-dimensional Ni_xCd_1- xS nanorods with enhanced visible-light response by ethanediamine-assisted decomposition of complex precursors, *J. Mater. Sci.*, **50**, 3920 (2015).
7. S. Dong, J. Feng, M. Fan, Y. Pi, L. Hu, X. Han, M. Liu, J. Sun, J. Sun, Recent developments in heterogeneous photocatalytic water treatment using visible light-responsive photocatalysts: a review, *Rsc Adv.*, **5**, 14610 (2015).
8. A. Primo, A. Corma, H. García, Titania supported gold nanoparticles as photocatalyst, *Phys. Chem. Chem. Phys.*, **13**, 886 (2011).
9. I. Tsuji, H. Kato, A. Kudo, Visible-Light-Induced H_2 Evolution from an Aqueous Solution Containing Sulfide and Sulfite over a ZnS–$CuInS_2$–$AgInS_2$ Solid-Solution Photocatalyst, *Angew. Chem.*, **44**, 3565 (2005).
10. J. Shen, J. Zai, Y. Yuan, X. Qian, 3D hierarchical $ZnIn_2S_4$: the preparation and photocatalytic properties on water splitting, *Int. J. Hydrog. Energy*, **37,** 16986 (2012).
11. A. Kudo, Y. Miseki, Heterogeneous photocatalyst materials for water splitting, *Chem. Soc. Rev.*, **38**, 253 (2009).
12. Y. Chen, H. Ge, L. Wei, Z. Li, R. Yuan, P. Liu, X. Fu, Reduction degree of reduced graphene oxide (RGO) dependence of photocatalytic hydrogen evolution performance over RGO/$ZnIn_2S_4$ nanocomposites, *Catal. Sci. Technol.*, **3**, 1712 (2013).
13. Z. Chen, D. Li, W. Zhang, C. Chen, W. Li, M. Sun, Y. He, X. Fu, Low-temperature and template-free synthesis of $ZnIn_2S_4$ microspheres, *Inorg. chem.*, **47**, 9766 (2008).
14. Z. Lei, W. You, M. Liu, G. Zhou, T. Takata, M. Hara, K. Domen, C. Li, Photocatalytic water reduction under visible light on a novel $ZnIn_2S_4$ catalyst synthesized by hydrothermal method, *ChemComm*, 2142 (2003).
15. I. Tsuji, H. Kato, H. Kobayashi, A. Kudo, Photocatalytic H_2 Evolution Reaction from Aqueous Solutions over Band Structure-Controlled $(AgIn)_xZn_2(1-x)S_2$ Solid Solution Photocatalysts with Visible-Light Response and Their Surface Nanostructures, *J. Am. Chem. Soc.*, **126**, 13406 (2004).
16. L. Ye, J. Fu, Z. Xu, R. Yuan, Z. Li, Facile one-pot solvothermal method to synthesize sheet-on-sheet reduced graphene oxide (RGO)/$ZnIn_2S_4$ nanocomposites with superior photocatalytic performance, *ACS appl. Mater. interfaces*, **6**, 3483 (2014).
17. J. Zhang, Y. Wang, J. Zhang, Z. Lin, F. Huang, J. Yu, Enhanced photocatalytic hydrogen production activities of Au-loaded ZnS flowers, *ACS appl. Mater. interfaces*, (2012).
18. Y. Chen, R. Huang, D. Chen, Y. Wang, W. Liu, X. Li, Z. Li, Exploring the different photocatalytic performance for dye degradations over hexagonal $ZnIn_2S_4$ microspheres and cubic $ZnIn_2S_4$ nanoparticles, *ACS appl. Mater. interfaces*, **4**, 2273 (2012).
19. S. Hemalatha, J.T. Illakkiya, R. Oommen, P.U. Rajalakshmi, Marigold microstructure of zinc thioindate ($ZnIn_2S_4$) thin film–Characteristics, *Optik*, **127**, 3858 (2016).
20. S.N. Habisreutinger, L. Schmidt-Mende, J.K. Stolarczyk, Photocatalytic reduction of CO_2 on TiO_2 and other semiconductors, *Angew. Chem.*, **52**, 7372 (2013).
21. J. Zhou, G. Tian, Y. Chen, X. Meng, Y. Shi, X. Cao, K. Pan, H. Fu, In situ controlled growth of $ZnIn_2S_4$ nanosheets on reduced graphene oxide for enhanced photocatalytic hydrogen production performance, *ChemComm*, **49,** 2237 (2013).
22. B. Kempken, V. Dzhagan, D.R. Zahn, M.J. Alcocer, I. Kriegel, F. Scotognella, J. Parisi, J. Kolny-Olesiak, Synthesis, optical properties, and

photochemical activity of zinc-indium-sulfide nanoplates, *RSC Adv.*, **5**, 89577 (2015).

23. Y. Chen, S. Hu, W. Liu, X. Chen, L. Wu, X. Wang, P. Liu, Z. Li, Controlled syntheses of cubic and hexagonal $ZnIn_2S_4$ nanostructures with different visible-light photocatalytic performance, *Dalton Trans.*, **40**, 2607 (2011).
24. W.-S. Seo, R. Otsuka, H. Okuno, M. Ohta, K. Koumoto, Thermoelectric properties of sintered polycrystalline $ZnIn_2S_4$, *J. Mater Res. Techno.*, **14**, 4176 (1999).
25. J. Chen, F. Xin, X. Yin, T. Xiang, Y. Wang, Synthesis of hexagonal and cubic $ZnIn_2S_4$ nanosheets for the photocatalytic reduction of CO_2 with methanol, *RSC Adv.*, **5**, 3833 (2015).
26. X. Gou, F. Cheng, Y. Shi, L. Zhang, S. Peng, J. Chen, P. Shen, Shape-controlled synthesis of ternary chalcogenide $ZnIn_2S_4$ and $CuIn(S,Se)_2$ nano-/microstructures via facile solution route, *J. Am. Chem. Soc.*, **128,** 7222 (2006).
27. L. Shi, P. Yin, Y. Dai, Synthesis and photocatalytic performance of $ZnIn_2S_4$ nanotubes and nanowires, *Langmuir*, **29**, 12818 (2013).
28. F. Fang, L. Chen, Y. B. Chen, L. M. Wu, Synthesis and photocatalysis of $ZnIn_2S_4$ nano/micropeony, *J. Phys. Chem. C*, **114**, 2393 (2010).
29. N.S. Chaudhari, A.P. Bhirud, R.S. Sonawane, L.K. Nikam, S.S. Warule, V.H. Rane, B.B. Kale, Ecofriendly hydrogen production from abundant hydrogen sulfide using solar light-driven hierarchical nanostructured $ZnIn_2S_4$ photocatalyst, *Green Chem.*, **13**, 2500 (2011).
30. B. Chai, T. Peng, P. Zeng, X. Zhang, X. Liu, Template-free hydrothermal synthesis of $ZnIn_2S_4$ floriated microsphere as an efficient photocatalyst for H_2 production under visible-light irradiation, *J. Phys. Chem. C*, **115**, 6149 (2011).
31. Z. Xu, Y. Li, S. Peng, G. Lu, S. Li, NaCl-assisted low temperature synthesis of layered Zn-In-S photocatalyst with high visible-light activity for hydrogen evolution, *RSC Adv.*, **2**, 3458 (2012).
32. R. Nomura, H. Matsuda, T. Miyai, A. Baba, Growth of spinel zinc thioindionate thin film by single-source MOCVD, *Thin Solid Films*, **342**, 108 (1999).
33. J. Yin, J. Jia, G. Yi, L. Wang, Preparation of $ZnIn_2S_4$ film electrodes by the SILAR technique, *J. Chin. Chem. Soc.*, **59**, 1365 (2012).
34. H. Yu, X. Quan, Y. Zhang, N. Ma, S. Chen, H. Zhao, Electrochemically assisted photocatalytic inactivation of Escherichia coli under visible light using a $ZnIn_2S_4$ film electrode, *Langmuir*, **24**, 7599 (2008).
35. K. W. Cheng, C. J. Liang, Preparation of Zn–In–S film electrodes using chemical bath deposition for photoelectrochemical applications, *Sol. Energy Mater Sol. Cells*, **94,** 1137 (2010).
36. P. Genevée, F. Donsanti, N. Schneider, D. Lincot, Atomic layer deposition of zinc indium sulfide films: Mechanistic studies and evidence of surface exchange reactions and diffusion processes, *J. Vac. Sci. Technol.*, **31**, 131 (2013).
37. S. Shen, J. Chen, X. Wang, L. Zhao, L. Guo, Microwave-assisted hydrothermal synthesis of transition-metal doped $ZnIn_2S_4$ and its photocatalytic activity for hydrogen evolution under visible light, *J. Power Sources*, **196,** 10112 (2011).
38. Y. Xie, Y. Liu, H. Cui, W. Zhao, C. Yang, F. Huang, Facile solution-based fabrication of $ZnIn_2S_4$ nanocrystalline thin films and their photoelectrochemical properties, *J. Power Sources*, **265,** 62 (2014).
39. M. Li, J. Su, L. Guo, Preparation and characterization of $ZnIn_2S_4$ thin films deposited by spray pyrolysis for hydrogen production, *Int. J. Hydrog. Energy.*, **33**, 2891 (2008).
40. J. Creighton, P. Ho, Introduction to chemical vapor deposition (CVD), *Chem. vap. Deposition*, **2**, 1 (2001).
41. C.E. Knapp, C.J. Carmalt, Solution based CVD of main group materials, *Chem. Soc. Rev.*, **45,** 1036 (2016).
42. M.A. Ehsan, T.N. Peiris, K.U. Wijayantha, M.M. Olmstead, Z. Arifin, M. Mazhar, K. Lo, V. McKee, Development of molecular precursors for deposition of indium sulphide thin film electrodes for photoelectrochemical applications, *Dalton Trans.*, **42,** 10919 (2013).
43. M.A. Ehsan, T.N. Peiris, K.U. Wijayantha, H. Khaledi, H.N. Ming, M. Misran, Z. Arifin, M. Mazhar, Surface morphological and photoelectrochemical studies of ZnS thin films developed from single source precursors by aerosol assisted chemical vapour deposition, *Thin Solid Films*, **540**, 1 (2013).
44. M.A. Ehsan, H.N. Ming, M. Misran, Z. Arifin, E.R. Tiekink, A.P. Safwan, M. Ebadi, W.J. Basirun, M. Mazhar, Effect of AACVD Processing Parameters on the Growth of Greenockite (CdS) Thin Films using a Single-Source Cadmium Precursor, *Chem. Vap. Deposition,* **18**, 191 (2012).
45. A.A. Tahir, M.A. Ehsan, M. Mazhar, K.U. Wijayantha, M. Zeller, A. Hunter,

Photoelectrochemical and photoresponsive properties of Bi_2S_3 nanotube and nanoparticle thin films, *Chem. Mater.*, **22**, 5084 (2010).

46. M.A. Ehsan, H. Khaledi, A.A. Tahir, H.N. Ming, K.U. Wijayantha, M. Mazhar, Synthesis and characterization of silver diethyldithiocarbamate cluster for the deposition of acanthite (Ag_2S) thin films for photoelectrochemical applications, *Thin Solid Films*, **536**, 124 (2013).
47. S. Chen, R.M.Wilson, R. Binions, Synthesis of highly surface-textured ZnO thin films by aerosol assisted chemical vapour deposition, *J. Mater. Chem. A.*, **3** (11), 5794-5797 (2015).
48. S. Chen, J. Wang, Z. Zhang, J. Briscoe, M. E. A. Warwick, H. Li, P. Hu,Aerosol assisted chemical vapour deposition of conformal ZnO compact layers for efficient elctron transport in perovskite solar cells, *Mater. Lett.*, **217**, 251-254 (2018).
49. M.A. Mansoor, M.A. Ehsan, V. McKee, N.-M. Huang, M. Ebadi, Z. Arifin, W.J. Basirun, M. Mazhar, Hexagonal structured $Zn_{(1-x)}Cd_xO$ solid solution thin films: synthesis, characterization and applications in photoelectrochemical water splitting, *J. Mater. Chem. A*, **1**, 5284 (2013).
50. Z, Zong, K, Liu, Z, Feng, Y, Bao, B, Dong, Hierarchical Sheet-on-Sheet $ZnIn_2S_4$/g-C_3N_4 Heterostructure with Highly Efficient Photocatalytic H_2 production Based on Photoinduced Interfacial Charge Transfer, *Sci. Rep.*, **6**, 19221(2016).
51. W. Cai, Y. Zhao, J. Hu, J. Zhong, W. Xiang, Solvothermal synthesis and characterization of zinc indium sulfide microspheres, *J. Mater. Sci. Technol.*, **27**, 559 (2011).
52. K. Otto, A. Katerski, O. Volobujeva, A. Mere, M. Krunks, Indium sulfide thin films deposited by chemical spray of aqueous and alcoholic solutions, *Energy Procedia*, **3**, 63 (2011).